HHS Public Access

Author manuscript

Hypertension. Author manuscript; available in PMC 2017 September 01.

Published in final edited form as:

Hypertension. 2016 September ; 68(3): 667–677. doi:10.1161/HYPERTENSIONAHA.116.07191.

Endothelial restoration of receptor activity-modifying protein 2 is sufficient to rescue lethality, but survivors develop dilated cardiomyopathy

Daniel O. Kechele[1], **William P. Dunworth**[2], **Claire E. Trincot**[2], **Sarah E. Wetzel-Strong**[1], **Manyu Li**[1], **Hong Ma**[3], **Jiandong Liu**[3], and **Kathleen M. Caron**[1,2]

[1]Department of Cell Biology and Physiology, The University of North Carolina, Chapel Hill, North Carolina, USA

[2]Curriculum in Genetics and Molecular Biology, The University of North Carolina, Chapel Hill, North Carolina, USA

[3]Department of Pathology and Laboratory Medicine, The University of North Carolina, Chapel Hill, North Carolina, USA

Abstract

Receptor activity-modifying proteins (RAMPs) serve as oligomeric modulators for numerous G protein-coupled receptors (GPCRs), yet elucidating the physiological relevance of these interactions remains complex. Receptor activity-modifying protein 2 (*Ramp2*) null mice are embryonic lethal, with cardiovascular developmental defects similar to those observed in mice null for canonical adrenomedullin/calcitonin receptor-like receptor (CLR) signaling. We aimed to genetically rescue the *Ramp2*$^{-/-}$ lethality in order to further delineate the spatiotemporal requirements for RAMP2 function during development and thereby enable the elucidation of an expanded repertoire of RAMP2 functions with Family B GPCRs in adult homeostasis. Endothelial-specific expression of *Ramp2* under the VE-cadherin promoter resulted in the partial rescue of *Ramp2*$^{-/-}$ mice, demonstrating that endothelial expression of *Ramp2* is necessary and sufficient for survival. The surviving *Ramp2*$^{-/-}$ *Tg* animals lived to adulthood and developed spontaneous hypotension and dilated cardiomyopathy, which was not observed in adult mice lacking CLR. Yet, the hearts of *Ramp2*$^{-/-}$ *Tg* animals displayed dysregulation of Family B GPCRs, including parathyroid hormone and glucagon receptors as well as their downstream signaling pathways. These data suggest a functional requirement for RAMP2 in the modulation of additional GPCR pathways *in vivo*, which is critical for sustained cardiovascular homeostasis. The cardiovascular importance of RAMP2 extends beyond the endothelium and canonical adrenomedullin/CLR signaling, in which future studies could elucidate novel and pharmacologically-tractable pathways for treating cardiovascular diseases.

Corresponding Author: Kathleen M. Caron, PhD, Professor and Chair, Department of Cell Biology and Physiology, 111 Mason Farm Road, 6312B Medical Biomolecular Research Building, CB# 7545, Chapel Hill, NC 27599, Fax: 919-843-1316, Telephone: 919-966-5193, kathleen_caron@med.unc.edu.

Conflicts of Interest/Disclosures: None

Keywords

RAMP; endothelium; dilated cardiomyopathy; GPCR; CLR; hypotension

Introduction

Receptor activity-modifying proteins (RAMPs) are single-pass transmembrane proteins that physically interact with numerous G protein-coupled receptors (GPCRs) to regulate receptor trafficking, ligand binding specificity and downstream G protein coupling and signaling. Biochemical and pharmacological studies have revealed functional RAMP interactions with many GPCRs including, calcitonin receptor-like receptor (CLR = protein, *Calcrl* = gene), calcitonin receptor (CTR), parathyroid hormone receptor 1 and 2 (PTHR1 and PTHR2), glucagon receptor (GCGR), secretin receptor (SCTR), vasointestinal peptide receptor 1 and 2 (VIPR1 and VIPR2), calcium sensing receptor (CaSR), an estrogen receptor (GPR30), and likely additional RAMP-interacting GPCRs will be identified in the future.[1–4] Thus, in their capacity as endogenous oligomeric GPCR partners, RAMPs can exert powerful modulation on nearly every aspect of GPCR function and on a wide range of physiological processes. However, our understanding regarding the complexity and consequences of RAMP-GPCR interactions *in vivo* lags behind our current structural, biochemical and pharmacological knowledge and thus presents a limitation toward harnessing the potential pharmacological utility of this family of proteins.

There exist three mammalian RAMPs, each encoded by single genes, which have been systematically knocked out by our laboratory and others.[5–7] As expected, based on their broad tissue distribution, the phenotypes of *Ramp* null mice are extensive and largely reflect their interactions with multiple GPCRs.[8] *Ramp1* and *Ramp3* null mice survive to adulthood, while *Ramp2*$^{-/-}$ mice exhibit embryonic lethality at mid-gestation due to cardiovascular defects in the heart, blood, and lymphatic vasculatures.[5–7, 9–11] These phenotypes are essentially identical to those observed in mice lacking the genes that encode for CLR and its Ramp2-associated ligand, adrenomedullin (AM), indicating that RAMP2 is essential for canonical CLR/AM signaling during embryonic development. Yet, mice that are haploinsufficient for *Ramp2* also exhibit an expanded constellation of endocrine-related phenotypes that are not observed in CLR and AM haploinsufficient mouse models.[12] Therefore, these data imply that RAMP2 must exert functional modulation of other GPCRs, which is supported by its *in vitro* biochemical interaction with CTR, PTHR1/2, GCGR, and VIPR1/2.[2] To date, ascribing a functional relevance for these other putative RAMP2-interacting GPCR pathways in adult physiological systems has been precluded by the embryonic lethality of *Ramp2*$^{-/-}$ mice.

Here, we have developed a novel *Ramp2* transgenic mouse model which overexpresses *Ramp2* specifically in the endothelium, with the hypothesis that restoration of RAMP2 in the endothelium will rescue the lethality-causing vascular defects associated with loss of CLR/AM signaling during embryogenesis. Indeed, endothelial RAMP2 is sufficient to rescue the embryonic lethality of many *Ramp2*$^{-/-}$ mice. Thus, the surviving mice, which express *Ramp2* in the endothelium but lack *Ramp2* in every other cell type, provided us with

the opportunity to further elucidate the functional implications of the loss of *Ramp2* on adult cardiovascular physiology and respective changes in other Ramp2-associated GPCRs.

Methods

Mouse Studies

Previously published SvEv-*Ramp2*$^{+/-}$ and *Calcrl*$^{flox/flox}$ mice were both fully backcrossed (>10 generations) onto a C57BL/6J genetic background for these studies.[5, 9] A novel endothelial-specific *Ramp2* transgenic mouse was generated and crossed to the *Ramp2*$^{+/-}$ mice. All *Ramp2* mice used in this study were maintained on an isogenic C57BL/6J genetic background. The *Calcrl*$^{flox/flox}$ mice were crossed with either the *SJL-Tg(Tagln-cre)1Her* (*SM22-Cre*) or the inducible *CAGG-CreER*^{TM} mouse to conditionally delete *Calcrl* specifically within developmental vascular smooth muscle cells (vSMC) or ubiquitously in adult mice, respectively. Adult *CAGG-CreER*^{TM} females were administered with tamoxifen (TAM) as previously published.[13] Genotyping and RT-PCR primers and probes are listed in Supplemental Table S1. Females between 4–8 months of age were used in all *Ramp2*-associated studies, males 3–4 months of age for vSMC-specific *Calcrl* studies, and females 16 month old for ubiquitous *Calcrl* studies. Mice were acclimated and conscious for both non-invasive tail cuff blood pressure and echocardiography analysis and anesthetized with isoflurane for intra-arterial blood pressure measurements. Organs weights and heart chamber dissections were normalized to either body weight or tibia length as previously described.[14] Biological N of 3–10 mice per genotype was used for each experiment. Endothelial cells from adult mice were isolated with magnetic-associated cell sorting using CD31-specific antibodies as previously described.[15] Cardiomyocytes from adult mice were isolated using collagenase digestion as previously described.[16] All animal experiments were approved by the Institutional Animal Care and Use Committee of The University of North Carolina at Chapel Hill.

Statistical Analysis

Statistical analysis was determined with GraphPad 5.0 and data is represented as mean ± SEM. The unpaired student T-test was used to compare two groups, while one way ANOVA with Tukey's Multiple Comparison test was used to compare 3 groups. Survival data were compared by Mantel-Cox and Gehan-Breslow-Wilcoxon tests. Significant differences are represented as * $p < 0.05$, ** $p < 0.01$, *** $p < 0.001$.

Additional detailed methods are provided in the Online Supplemental Data.

Results

Generation and Characterization of Endothelial-Specific Ramp2 Transgenic Animals

A diagram of the *Cdh5-Ramp2* transgene (Tg) depicts the murine vascular cadherin 5 (Cdh5) promoter driving the expression of a flagged-tagged murine *Ramp2* cDNA (Supplemental Figure S1A), which was successfully integrated into the genome of two independent founder lines on the C57BL/6J genetic background. Expression of FLAG-Ramp2 protein was confirmed using both transgenic founder lines in a variety of adult

tissues including the heart, kidney, lung and intestine (Supplemental Figure S1B). Semi-quantitative RT-PCR revealed the presence of *FLAG* transcript within whole adult lung tissue and CD31+ endothelial-enriched cells in the *Tg* animals, but not wildtype endothelium (Supplemental Figure S1C), which resulted in a modest increase in overall *Ramp2* gene expression levels within lung CD31+ endothelial cells of *Tg* animals compared to wildtype animals (Supplemental Figure S1D). *Ramp2* expression was significantly higher in the left ventricles of *Tg* animals compared to wild-type—a finding which we attribute to the endothelial-driven transgene expression, as compared to the low levels of endogenous *Ramp2* expression in isolated cardiomyocytes (Supplemental Figure S1E) and previously reported expression in vSMCs.[17, 18] *Tg(Cdh5-Ramp2)* mice bred normally, with expected Mendelian and sex ratios at birth, and no obvious phenotypic defects.

Transgenic Endothelial Ramp2 Partially Rescues Embryonic Lethality of Ramp2$^{-/-}$ Mice

We sought to determine whether endothelial *Ramp2* expression could rescue the previously reported *Ramp2*$^{-/-}$ embryonic lethality by interbreeding the hemizygous *Tg(Cdh5-Ramp2)* animals with *Ramp2*$^{+/-}$ non-transgenic (ntg) animals, on an isogenic C57BL/6J genetic background.[7, 9] *Ramp2*$^{+/-}$ *Tg(Cdh5-Ramp2)* mice (hereafter referred to as *Ramp2*$^{+/-}$ *Tg)* were crossed to *Ramp2*$^{+/-}$ *ntg* animals to generate *Ramp2*$^{-/-}$ embryos with or without expression of the transgene. At e14.5, all six possible genotypes were observed (Supplemental Figure S2A). As expected, embryos lacking *Ramp2* display non-hemorrhagic edema associated with arrested lymphangiogenesis,[9] yet the *Ramp2*$^{-/-}$ *Tg* embryos showed significantly less edema than *Ramp2*$^{-/-}$ *ntg* littermates (Figure 1A–B). Unlike the small, hypoplastic jugular lymph sacs of *Ramp2*$^{-/-}$ *ntg* embryos, the jugular lymph sacs of the *Ramp2*$^{-/-}$ *Tg* were comparable in size to those of *Ramp2*$^{+/+}$ littermates (Figure 1C–D), demonstrating that transgenic restoration of functional *Ramp2* in the endothelium leads to improvement of the edematous phenotype.

In addition to defects in lymphatic development, loss of *Ramp2* or AM/CLR signaling leads to small, disorganized hearts and thin vSMC walls.[9, 19, 20] The aortic endothelium of viable embryos appeared intact with no signs of hemorrhagic leakage or endothelial dysfunction as previously reported in some *Ramp2*$^{-/-}$ embryos.[7] However, the aortic vSMC layer was significantly thinner in *Ramp2*$^{-/-}$ *ntg* and *Ramp2*$^{-/-}$ *Tg* embryos (Figure 1E–F). Likewise, the hearts of e14.5 *Ramp2*$^{-/-}$ *Tg* animals were comparable in size to *Ramp2*$^{-/-}$ *ntg* littermates, which were both significantly smaller than controls, despite detectable expression of *Ramp2* in *Ramp2*$^{-/-}$ *Tg* hearts (Figure 1G–I). Consistent with previous reports, these data reflect that Ramp2 expression is required for normal vSMC and cardiac development and that endothelial *Ramp2* restoration is not sufficient to rescue these defects, thus confirming non-endothelial roles of Ramp2 during cardiovascular development.

Unlike the *Ramp2*$^{-/-}$ *ntg* embryos, which uniformly die by e15.5, *Ramp2*$^{-/-}$ *Tg* embryos survive to term at near-Mendelian ratios, but a large number of these animals were found stillborn at postnatal day 1 (Supplemental Figure S2B). Nevertheless, by postnatal day 7, 40% of the expected Mendelian ratio of *Ramp2*$^{-/-}$ *Tg* pups were viable, which represents a significant survival rescue when compared to the completely penetrant lethality of *Ramp2*$^{-/-}$ *ntg* mice (Table 1). These surviving *Ramp2*$^{-/-}$ *Tg* mice were indistinguishable from

Ramp2$^{+/+}$ littermates (Supplemental Figure S2C). Interestingly, there was a significant skewing in the sex ratio of the surviving *Ramp2*$^{-/-}$ *Tg* mice, such that 78% were female. These data demonstrate that transgenic endothelial restoration of *Ramp2* is able to blunt the endothelial and edematous phenotypes observed with global *Ramp2* genetic deletion, leading to significantly improved survival.

Surviving Ramp2$^{-/-}$ Tg Adult Mice are Hypotensive

The surviving *Ramp2*$^{-/-}$ *Tg* mice, which express *Ramp2* in the endothelium but lack *Ramp2* in all other cells, provided an opportunity to evaluate how Ramp2 loss-of-function during development affects adult cardiovascular homeostasis. Diastolic, systolic, and mean arterial blood pressures were significantly reduced in *Ramp2*$^{-/-}$ *Tg* compared to *Ramp2*$^{+/+}$ *ntg* and *Tg* female controls (Figure 2A). Importantly, there were no significant differences in basal blood pressure between *Ramp2*$^{+/+}$ *ntg* and *Ramp2*$^{+/+}$ *Tg* mice, indicating that the decreased blood pressure was not caused solely by the transgene. Moreover, the reduced basal blood pressure of *Ramp2*$^{-/-}$ *Tg* mice was observed without the exogenous administration of the canonical, hypotensive ligand AM, which was previously required to lower blood pressures in a vSMC-specific overexpression model of *Ramp2*.[21, 22]

Similar to the developmental defects in vSMC wall thickness of the *Ramp2*$^{-/-}$ *Tg* embryos and other models lacking AM/CLR/Ramp2 function,[9, 19, 20] the vSMC walls were significantly thinner in *Ramp2*$^{-/-}$ *Tg* adult descending aortas compared to wild-type controls (Figure 2B). Intra-arterial blood pressure measurements further confirmed the hypotensive phenotype of adult *Ramp2*$^{-/-}$ *Tg* females (Figure 2C). To test vSMC responsiveness, *Ramp2*$^{-/-}$ *Tg* and controls were challenged with intravenous injections of the α-adrenergic receptor agonist, phenylephrine, and the vasodilator, AM. The *Ramp2*$^{-/-}$ *Tg* adults were capable of normal vasoconstriction and vasodilation as compared to controls (Figure 2C). So, although the thinner vSMC walls likely play a role in the hypotensive phenotype of *Ramp2*$^{-/-}$ *Tg* mice, additional systemic changes likely contribute to the hypotension.

Ramp2$^{-/-}$ Tg Mice Develop Spontaneous Dilated Cardiomyopathy Phenotype

Considering the hypotension and the developmental defects observed in *Ramp2*$^{-/-}$ *Tg* embryonic hearts, we next assessed how cardiac function and morphology were altered in adult *Ramp2*$^{-/-}$ *Tg* mice. Echocardiography on conscious mice revealed significantly dilated left ventricles during both diastole and systole, with significantly larger left ventricle volumes and left ventricle internal diameter dimensions in the *Ramp2*$^{-/-}$ *Tg* mice compared to *Ramp2*$^{+/+}$ and *Ramp2*$^{+/-}$, with and without the transgene (Table 2). Representative M-mode echocardiograms from *Ramp2*$^{+/+}$ *ntg*, *Ramp2*$^{+/+}$ *Tg*, and *Ramp2*$^{-/-}$ *Tg* illustrate the ventricular dilation in *Ramp2*$^{-/-}$ *Tg* mice (Figure 3A), which resulted in a trending increase in calculated cardiac output in these animals (Table 2). Septum and left ventricle posterior wall dimensions of *Ramp2*$^{-/-}$ *Tg* mice were unchanged from controls, although there was a non-significant trend towards a thinner posterior wall. There was also a modest, but significant reduction in both ejection fraction and fractional shortening in the *Ramp2*$^{-/-}$ *Tg* dilated hearts. These data indicate that loss of *Ramp2* in non-endothelial cells leads to a spontaneous dilated cardiomyopathy (DCM)–like phenotype in adult mice, which at 6

months of age had not yet progressed to heart failure, as indicated by the elevated cardiac output and sufficient heart function.

Upon dissection, we observed that the hearts of *Ramp2*$^{-/-}$ *Tg* mice were grossly enlarged compared to wildtype and *Ramp2*$^{-/-}$ *ntg* mice (Figure 3B–C). The adult *Tg* mice had no differences in body weight (*Ramp2*$^{+/+}$ *ntg*: 28.4 ± 1.4 g, *Ramp2*$^{+/+}$ *Tg*: 28.4 ± 1.2 g, *Ramp2*$^{-/-}$ *Tg*: 28.3 ± 1.2 g) or tibia length (*Ramp2*$^{+/+}$ *ntg*: 17.6 ± 0.2 mm, *Ramp2*$^{+/+}$ *Tg*: 17.9 ± 0.1 mm, *Ramp2*$^{-/-}$ *Tg*: 17.8 ± 0.2 mm) regardless of their *Ramp2* genotype. Yet, total heart weights were significantly larger in the *Ramp2*$^{-/-}$ *Tg* mice when normalized to both body weight (Figure 3D) or tibia length (R*amp2*$^{+/+}$ *ntg*: 7.3 ± 0.4 mg/mm, *Ramp2*$^{+/+}$ *Tg*: 6.5 ± 0.2 mg/mm, *Ramp2*$^{-/-}$ *Tg*: 9.0 ± 0.3** mg/mm; **p<0.01). Moreover, when normalized to body weight the left ventricle (Figure 3E), right ventricle (Figure 3F), and right atria (*Ramp2*$^{+/+}$ *ntg*: 0.15 ± 0.01 mg/g, *Ramp2*$^{+/+}$ *Tg*: 0.15 ± 0.01 mg/g, *Ramp2*$^{-/-}$ *Tg*: 0.21 ± 0.02* mg/g; *p<0.05) all exhibited significant enlargement in the *Ramp2*$^{-/-}$ *Tg* animals compared to all other genotypes. Similar significant trends were observed when the individual chamber weights were normalized to tibia length (LV:TL; *Ramp2*$^{+/+}$ *ntg*: 5.4 ± 0.3 mg/mm, *Ramp2*$^{+/+}$ *Tg*: 4.8 ± 0.2 mg/mm, *Ramp2*$^{-/-}$ *Tg*: 6.5 ± 0.2** mg/mm; **p<0.01).

Cross-sectional area of myocytes within the left ventricle revealed slight, but significant cardiomyocyte hypertrophy, with no changes in left ventricular capillary density, in the *Ramp2*$^{-/-}$ *Tg* mice compared to controls (Figure 4A–D). Picrosirius red staining showed no differences in perivascular fibrosis, but there was significantly increased interstitial fibrosis in the *Ramp2*$^{-/-}$ *Tg* hearts compared to hearts of *Ramp2*$^{+/+}$ and *Ramp2*$^{+/+}$ *Tg* mice (Figure 4E–H). There were elevated levels of the oxidative stress indicator, lipid peroxidase evidenced by 4-hydroxynonenal (4-HNE) staining in *Ramp2*$^{-/-}$ *Tg* hearts (Figure 4I–J).[23] Together, the modest increases in hypertrophy, fibrosis, and oxidative stress, as well as modest decline in heart function, further support that 6 month old *Ramp2*$^{-/-}$ *Tg* mice exhibit a compensated, DCM-like phenotype.

Adult Ramp2$^{-/-}$ Tg Mice Develop Multi-Organ Inflammation

DCM and hypotension can lead to vascular congestion and organ dysfunction throughout the body.[24–26] Consistently, we observed that the spleen to body weight ratio was significantly increased in the *Ramp2*$^{-/-}$ *Tg* mice compared to all other genotypes (Figure 5A). *Ramp2*$^{-/-}$ *Tg* mice also exhibited macroscopic vascular congestion within their livers compared to control animals (Figure 5B). Furthermore, multi-organ histology revealed a marked increase in the number of inflammatory foci, particularly surrounding the vasculature, within the liver (Figure 5C–D), kidney (Figure 5E–F) and lungs (Figure 5G–H). A diagnostic profile of adult serum from wildtype and *Ramp2*$^{-/-}$ *Tg* mice revealed few significant changes in circulating ions or enzyme levels that are typically indicative of hepatocellular or renal damage (Supplemental Table S2). This supports that the end-organ inflammation in *Ramp2*$^{-/-}$ *Tg* mice is likely downstream of altered hemodynamics due to DCM and hypotension, rather than primarily due to loss-of-function of Ramp2 in end-organs.

Conditional Calcrl Deletion Does Not Lead to a Dilated Cardiomyopathy Phenotype

Since CLR and AM represent the most well-characterized, canonical pathway for RAMP2 modulation and the knockout mice for these genes recapitulate the *Ramp2*$^{-/-}$ developmental phenotypes, it is reasonable to consider that disruption of this pathway, which has been demonstrated to be cardioprotective in both animal studies and in humans,[27–30] may underlie the DCM and hypotensive phenotypes in *Ramp2*$^{-/-}$ *Tg* mice. To test the functions of CLR in non-endothelial cells, we generated cardiac- and vSMC-specific *Calcrl* null mice using the SM22-Cre mediated excision. The *Calcrl*$^{loxP/loxP}$*; SM22Cre+* mice were born at expected Mendelian ratios and survived to adulthood (Supplemental Figure S3A). Relative *Calcrl* expression was significantly reduced in aortic vSMCs and hearts of *Calcrl*$^{loxP/loxP}$*; SM22-Cre+* compared to *Calcrl*$^{loxP/+}$*; SM22-Cre+* littermates (Supplemental Figure S3B). Importantly, *Calcrl*$^{loxP/loxP}$*; SM22*-Cre+ adult males were normotensive and had no basal changes in heart function, size, or morphology (Supplemental Table S3 or Figure S3C). Similarly, cardiac-specific *Calcrl* deletion using the *αMHC-Cre+* transgenic line also failed to recapitulate the DCM phenotype, with animals surviving to adulthood with no basal cardiac dysfunction (Dackor R & Caron K.M., unpublished data, [2016]). These data demonstrate that cardiac- and vSMC-specific *Calcrl* expression is not required for embryonic development or adult cardiovascular maintenance.

We have previously shown that temporal, global deletion of *Calcrl* in adult *Calcrl*$^{loxP/loxP}$; *CAGG-CreER*^{TM} mice results in dilated lymphangiectasia in many lymphatic vascular beds throughout the body.[13] However, these mice did not display any obvious cardiac phenotypes and they had similar heart to body weight ratio as TAM-injected control mice (*Calcrl*$^{loxP/loxP}$; *CAGG-CreER*^{TM}: 4.43 ± 0.19 mg/g versus *Calcrl*$^{flox/flox}$: 4.13 ± 0.14 mg/g, respectively). Furthermore, conscious echocardiography of *Calcrl*$^{loxP/loxP}$; *CAGG-CreER*^{TM} female mice, even at 14 months of age, failed to reveal any significant changes in left ventricle internal diameter, function, or heart size compared to control mice (Supplemental Table S4). Collectively, these data, generated from three independent series of conditional deletion approaches, indicate that the global-, cardiac- or vSMC-specific loss of *Calcrl* does not recapitulate the DCM phenotype observed in the *Ramp2*$^{-/-}$ *Tg* animals. Therefore, this strongly suggests that the *Ramp2*$^{-/-}$ *Tg* phenotype is imparted by other RAMP2-associated GPCR pathways.

Ramp2$^{-/-}$ Tg hearts exhibit reduced signaling pathways and expression of numerous RAMP-associated GPCRs

The genetic reduction or down-regulation of the transcriptional regulator CREB[25, 31] and the crucial PPAR pathway transcription factor, *Pgc-1α*,[32–34] have both been shown to be involved in DCM pathogenesis. Thus as expected, the relative expression of *Pgc-1α* was significantly down-regulated in left ventricles and in an enriched cardiomyocytes fraction of *Ramp2*$^{-/-}$ *Tg* hearts compared to controls (Figure 6A–B). There was also a significant reduction in phosphorylated CREB compared to total CREB and Gapdh in the *Ramp2*$^{-/-}$ *Tg* hearts compared to *Ramp2*$^{+/+}$ *ntg* and *Ramp2*$^{+/+}$ *Tg* hearts (Figure 6C). Numerous Family B GPCRs signal through these pathways, including the Gcgr which has been shown to signal through cAMP to activate both CREB and PPAR transcription,[35–38] and both the Pthr1 and CaSR signal through cAMP and CREB.[39–41] Interestingly, the gene expression levels of

these RAMP-associated GPCRs were significantly down-regulated in the left ventricles of *Ramp2*$^{-/-}$ *Tg* mice compared to those of control animals, whereas genes encoding for other RAMP-associated GPCRs, like *Calcr*, *Vipr1*, and *Gpr30*, were unchanged (Figure 6D).

Similar gene expression changes in these Family B GPCR expression profiles were confirmed in isolated cardiomyocyte fractions (Figure 6E), further supporting the myocyte-specific genetic dysregulation. *Calcrl* expression was significantly increased in left ventricle, but not in the cardiomyocyte-enriched fraction, demonstrating that *Calcrl* upregulation is from a non-cardiomyocyte cell type. The expression of both *Pthr1* and *Gcgr* were significantly decreased during development in the hearts of *Ramp2*$^{-/-}$ *ntg* and *Ramp2*$^{-/-}$ *Tg* embryos (Figure 6F), supporting that these changes are specific to *Ramp2* loss rather than secondary to the Cdh5-driven *Ramp2 Tg* or the DCM phenotype, as might be the case for *CaSR*. Serum analysis revealed no significant dysregulation of circulating calcium or glucose, thereby eliminating uncompensated Pthr1 or Gcgr systemic signaling as a cause for the cardiovascular phenotypes (Supplemental Table S2). Collectively, these data demonstrate that genetic loss of *Ramp2* in non-endothelial cells of the heart leads to down-regulation of both RAMP2-associated GPCRs, *Gcgr* and *Pthr1*, as an underlying mechanistic basis for the decreased pCREB and *Pgc-1α* responsible for the pathogenesis of the DCM-like phenotype in *Ramp2*$^{-/-}$ *Tg* mice (Figure 6G).

Discussion

In this study, we generated an endothelial-specific *Ramp2 Tg* mouse model to attempt to rescue the embryonic lethality due to global loss of *Ramp2*. While no *Ramp2* null mice survive to birth, we observed a significant number of *Ramp2*$^{-/-}$ *Tg* born and able to survive into adulthood. This result further confirms that endothelial *Ramp2* is essential for embryonic survival and represents, to our knowledge, the first genetic rescue of the global *Ramp2* null lethality.

It remains unclear why a significant number of Ramp2$^{-/-}$ Tg pups survive to late-gestation, but are stillborn. Interestingly, it was recently shown that mice with endothelial excision of *Ramp2* during development using a *Cdh5-Cre* died during late-gestation.[24] Additionally, they report that approximately 5% of the endothelial *Ramp2* knockouts live into adulthood and develop large hearts, hypotension, and multi-organ vasculitis. In this current study we found that 40% of *Ramp2*$^{-/-}$ *Tg* survived to adulthood, and also developed similar cardiovascular and inflammatory phenotypes. These two mouse models, as well as a previously published endothelial-specific deletion of *Calcrl*, demonstrate that adequate levels and timing of endothelial Ramp2/CLR/AM signaling are critical for embryonic survival.[9]

In addition, these studies identify potential sex-dependent mechanisms of Ramp2, or Cdh5, regulation and function, as evidenced by the substantially reduced numbers of male *Ramp2*$^{-/-}$ *Tg* survivors. We have previously shown that adult *Ramp2*$^{+/-}$ females have endocrine phenotypes not present in *Ramp2*$^{+/-}$ males.[12] In addition, *Ramp3*$^{-/-}$ males, but not females, displayed exacerbated cardiovascular phenotypes when challenged with hypertension.[4, 10] Thus, while RAMP2 and RAMP3 interact with both similar and different

GPCRs, our observations of sex-dependent phenotypes in these genetic animals will provide an area for interesting future investigations.

The complex compensatory mechanisms through which RAMP-mediated AM/CLR signaling regulate blood pressure have not been fully elucidated. It is well documented that AM infusion acts to lower blood pressure through both vSMC and endothelium, but it remains disputed if altered AM expression using genetic models alters basal blood pressure.[18, 42–45] Moreover, while developmental loss of *Ramp2* leads to spontaneous hypotension and adult *Ramp1*$^{-/-}$ mice develop hypertension.[11, 24] *Calcrl* deletion in vSMC and cardiomyocytes appears dispensable for regulation of basal vascular tone in adult males. It is evident that Ramp2 and AM signaling plays a role in vSMC and myocardium development and function, which likely contributes to the pathogenesis of hypotension and DCM in *Ramp2*$^{-/-}$ *Tg* survivors. Yet, the hypotension and DCM phenotypes occur despite maintenance of normal cardiac output. It is further possible that the developmentally-induced thin vSMC walls contribute to reduced vascular tone; however we demonstrated their ability to effectively respond to acute phenylephrine vasoconstriction. Therefore, additional studies that explore the entire repertoire of RAMP-mediated GPCRs will be required for full elucidation of the mechanistic basis for the hypotension in *Ramp2*$^{-/-}$ *Tg* survivors.

Loss of *Ramp2* in multiple non-endothelial cardiac cells, along with altered humoral signaling could lead to cardiac dysfunction and DCM pathogenesis. The genetic dysregulation in isolated cardiomyocytes suggests roles of Ramp2/GPCRs specifically in cardiomyocytes. Interestingly, a recently published study demonstrated that a cardiomyocyte-specific *Ramp2* deletion led to a DCM-like phenotype due to mitochondrial dysfunction and irregular calcium handling, which the authors attribute to loss of CLR/AM signaling.[46] Similarly, this study suggests that cardiomyocyte loss of *Ramp2* in the *Ramp2*$^{-/-}$ *Tg* mice is likely responsible for the DCM. Moreover, our data demonstrates that neither cardiomyocyte- or vSMC-specific loss of *Calcrl* during development or conditional *Calcrl* deletion in adults recapitulate the DCM phenotype observed in the *Ramp2*$^{-/-}$ *Tg* and the aforementioned *Ramp2*$^{flox/flox}$; α*MHC-MerCreMer* mice.[46] Therefore, collectively, these studies imply the involvement of other RAMP-associated GPCRs.

It is apparent that RAMPs interact with numerous GPCRs biochemically, although *in vivo* physiologic evidence of these interactions is limited. We found that lack of *Ramp2* in non-endothelial cells leads to decreased expression of cardiac *Pthr1* and *Gcgr.* Interestingly, human PTHR1 and GCGR interact specifically with RAMP2 and not RAMP1 or RAMP3 in which RAMP2 is important in chaperoning both GPCRs to the plasma membrane.[2] Furthermore, it was recently demonstrated that RAMP2 was important in GCGR ligand selectivity between glucagon and glucagon-like peptide 1, which have opposing physiologic effects on glucose homeostasis and cardiovascular function.[47] While GCGR has not been directly connected to DCM pathogenesis, glucagon can alter calcium signaling in myocytes and glucagon-like peptide 1 improves glucose uptake and survival of canines with DCM.[35, 48] Likewise PTHR1 signaling is important in vitamin D and calcium homeostasis, which have both been associated with DCM.[49, 50] Together, *Ramp2* loss-of-function can not only alter both *Pthr1* and *Gcgr* expression simultaneously, but may also alter their ability to

reach plasma membrane, bind ligands, and signal. Additionally, we observed decreased signaling through CREB and downregulation of *Pgc-1a*, which both have been shown to lead to DCM.[25, 31, 32] Both Pthr1 and Gcgr signal through CREB and murine deletion of *Gcgr* led to decreased phosphorylated CREB and *Pgc-1a* expression levels.[36, 38] Thus, loss of *Ramp2* likely has numerous mechanisms for the development and maintenance of cardiac functions both dependent and independent of canonical AM/CLR/Ramp2 signaling.

Perspectives

The *in vivo* interplay between GPCR/RAMP/Ligand is highly complex and is only starting to be understood. However, a better understanding of these interactions in a spatial and temporal manner in a pathophysiologic context will help us better target the unique GPCR/RAMP interfaces to potentially treat disease like DCM and hypertension.

Supplementary Material

Refer to Web version on PubMed Central for supplementary material.

Acknowledgments

We thank the University of North Carolina Animal Models Core, the University of North Carolina Rodents Advanced Surgical Models Core, the University of North Carolina Histology Research Core, and the University of North Carolina Lineberger Animal Histopathology Core (NIH CA16086). We also thank Dr. Lin Xiao, Dr. Andrew Dudley, Dr. Samantha Hoopes, John Pawlak and other members of Caron laboratory for technical support and discussions.

Sources of Funding

This work was supported by NIH HL091973, HD060860, and DK099156 grants to K.M.C.; NIH F31-CA174194 and the University of North Carolina Cell and Molecular Physiology Fellner Fellowship to D.O.K.; an American Heart Association 12PRE11710002 to S.E.W-S.; and an American Heart Association 15PRE25680001 to C.E.T.

References

1. McLatchie LM, Fraser NJ, Main MJ, Wise A, Brown J, Thompson N, Solari R, Lee MG, Foord SM. RAMPs regulate the transport and ligand specificity of the calcitonin-receptor-like receptor. Nature. 1998; 393:333–339. [PubMed: 9620797]
2. Christopoulos A, Christopoulos G, Morfis M, Udawela M, Laburthe M, Couvineau A, Kuwasako K, Tilakaratne N, Sexton PM. Novel receptor partners and function of receptor activity-modifying proteins. J Biol Chem. 2003; 278:3293–3297. [PubMed: 12446722]
3. Bouschet T, Martin S, Henley JM. Receptor-activity-modifying proteins are required for forward trafficking of the calcium-sensing receptor to the plasma membrane. J Cell Sci. 2005; 118:4709–4720. [PubMed: 16188935]
4. Lenhart PM, Broselid S, Barrick CJ, Leeb-Lundberg LM, Caron KM. G-protein-coupled receptor 30 interacts with receptor activity-modifying protein 3 and confers sex-dependent cardioprotection. J Mol Endocrinol. 2013; 51:191–202. [PubMed: 23674134]
5. Dackor R, Fritz-Six K, Smithies O, Caron K. Receptor activity-modifying proteins 2 and 3 have distinct physiological functions from embryogenesis to old age. J Biol Chem. 2007; 282:18094–18099. [PubMed: 17470425]
6. Li M, Wetzel-Strong SE, Hua X, Tilley SL, Oswald E, Krummel MF, Caron KM. Deficiency of RAMP1 attenuates antigen-induced airway hyperresponsiveness in mice. PLoS One. 2014; 9:e102356. [PubMed: 25010197]

7. Ichikawa-Shindo Y, Sakurai T, Kamiyoshi A, Kawate H, Iinuma N, Yoshizawa T, Koyama T, Fukuchi J, Iimuro S, Moriyama N, Kawakami H, Murata T, Kangawa K, Nagai R, Shindo T. The GPCR modulator protein RAMP2 is essential for angiogenesis and vascular integrity. J Clin Invest. 2008; 118:29–39. [PubMed: 18097473]
8. Kadmiel M, Fritz-Six KL, Caron KM. Understanding RAMPs through genetically engineered mouse models. Adv Exp Med Biol. 2012; 744:49–60. [PubMed: 22434107]
9. Fritz-Six KL, Dunworth WP, Li M, Caron KM. Adrenomedullin signaling is necessary for murine lymphatic vascular development. J Clin Invest. 2008; 118:40–50. [PubMed: 18097475]
10. Barrick CJ, Lenhart PM, Dackor RT, Nagle E, Caron KM. Loss of receptor activity-modifying protein 3 exacerbates cardiac hypertrophy and transition to heart failure in a sex-dependent manner. J Mol Cell Cardiol. 2012; 52:165–174. [PubMed: 22100352]
11. Tsujikawa K, Yayama K, Hayashi T, et al. Hypertension and dysregulated proinflammatory cytokine production in receptor activity-modifying protein 1-deficient mice. Proc Natl Acad Sci U S A. 2007; 104:16702–16707. [PubMed: 17923674]
12. Kadmiel M, Fritz-Six K, Pacharne S, Richards GO, Li M, Skerry TM, Caron KM. Research resource: Haploinsufficiency of receptor activity-modifying protein-2 (RAMP2) causes reduced fertility, hyperprolactinemia, skeletal abnormalities, and endocrine dysfunction in mice. Mol Endocrinol. 2011; 25:1244–1253. [PubMed: 21566080]
13. Hoopes SL, Willcockson HH, Caron KM. Characteristics of multi-organ lymphangiectasia resulting from temporal deletion of calcitonin receptor-like receptor in adult mice. PLoS One. 2012; 7:e45261. [PubMed: 23028890]
14. Wetzel-Strong SE, Li M, Klein KR, Nishikimi T, Caron KM. Epicardial-derived adrenomedullin drives cardiac hyperplasia during embryogenesis. Dev Dyn. 2014; 243:243–256. [PubMed: 24123312]
15. Xiao L, Harrell JC, Perou CM, Dudley AC. Identification of a stable molecular signature in mammary tumor endothelial cells that persists in vitro. Angiogenesis. 2014; 17:511–518. [PubMed: 24257808]
16. Qian L, Huang Y, Spencer CI, Foley A, Vedantham V, Liu L, Conway SJ, Fu JD, Srivastava D. In vivo reprogramming of murine cardiac fibroblasts into induced cardiomyocytes. Nature. 2012; 485:593–598. [PubMed: 22522929]
17. Oie E, Vinge LE, Andersen GO, Yndestad A, Krobert KA, Sandberg C, Ahmed MS, Haug T, Levy FO, Skomedal T, Attramadal H. RAMP2 and RAMP3 mRNA levels are increased in failing rat cardiomyocytes and associated with increased responsiveness to adrenomedullin. J Mol Cell Cardiol. 2005; 38:145–151. [PubMed: 15623431]
18. Nishimatsu H, Suzuki E, Nagata D, Moriyama N, Satonaka H, Walsh K, Sata M, Kangawa K, Matsuo H, Goto A, Kitamura T, Hirata Y. Adrenomedullin induces endothelium-dependent vasorelaxation via the phosphatidylinositol 3-kinase/Akt-dependent pathway in rat aorta. Circ Res. 2001; 89:63–70. [PubMed: 11440979]
19. Caron KM, Smithies O. Extreme hydrops fetalis and cardiovascular abnormalities in mice lacking a functional Adrenomedullin gene. Proc Natl Acad Sci U S A. 2001; 98:615–619. [PubMed: 11149956]
20. Dackor RT, Fritz-Six K, Dunworth WP, Gibbons CL, Smithies O, Caron KM. Hydrops fetalis, cardiovascular defects, and embryonic lethality in mice lacking the calcitonin receptor-like receptor gene. Mol Cell Biol. 2006; 26:2511–2518. [PubMed: 16537897]
21. Tam CW, Husmann K, Clark NC, et al. Enhanced vascular responses to adrenomedullin in mice overexpressing receptor-activity-modifying protein 2. Circ Res. 2006; 98:262–270. [PubMed: 16373602]
22. Liang L, Tam CW, Pozsgai G, Siow R, Clark N, Keeble J, Husmann K, Born W, Fischer JA, Poston R, Shah A, Brain SD. Protection of angiotensin II-induced vascular hypertrophy in vascular smooth muscle-targeted receptor activity-modifying protein 2 transgenic mice. Hypertension. 2009; 54:1254–1261. [PubMed: 19858409]
23. Dalleau S, Baradat M, Gueraud F, Huc L. Cell death and diseases related to oxidative stress: 4-hydroxynonenal (HNE) in the balance. Cell Death Differ. 2013; 20:1615–1630. [PubMed: 24096871]

24. Koyama T, Ochoa-Callejero L, Sakurai T, et al. Vascular endothelial adrenomedullin-RAMP2 system is essential for vascular integrity and organ homeostasis. Circulation. 2013; 127:842–853. [PubMed: 23355623]
25. Fentzke RC, Korcarz CE, Lang RM, Lin H, Leiden JM. Dilated cardiomyopathy in transgenic mice expressing a dominant-negative CREB transcription factor in the heart. J Clin Invest. 1998; 101:2415–2426. [PubMed: 9616213]
26. Minamishima YA, Moslehi J, Bardeesy N, Cullen D, Bronson RT, Kaelin WG Jr. Somatic inactivation of the PHD2 prolyl hydroxylase causes polycythemia and congestive heart failure. Blood. 2008; 111:3236–3244. [PubMed: 18096761]
27. Shimosawa T, Shibagaki Y, Ishibashi K, Kitamura K, Kangawa K, Kato S, Ando K, Fujita T. Adrenomedullin, an endogenous peptide, counteracts cardiovascular damage. Circulation. 2002; 105:106–111. [PubMed: 11772884]
28. Eto T, Kitamura K, Kato J. Biological and clinical roles of adrenomedullin in circulation control and cardiovascular diseases. Clin Exp Pharmacol Physiol. 1999; 26:371–380. [PubMed: 10386225]
29. Nishikimi T, Yoshihara F, Horinaka S, Kobayashi N, Mori Y, Tadokoro K, Akimoto K, Minamino N, Kangawa K, Matsuoka H. Chronic administration of adrenomedullin attenuates transition from left ventricular hypertrophy to heart failure in rats. Hypertension. 2003; 42:1034–1041. [PubMed: 14568998]
30. Nishikimi T, Yoshihara F, Mori Y, Kangawa K, Matsuoka H. Cardioprotective effect of adrenomedullin in heart failure. Hypertens Res. 2003; 26(Suppl):S121–127. [PubMed: 12630822]
31. Watson PA, Birdsey N, Huggins GS, Svensson E, Heppe D, Knaub L. Cardiac-specific overexpression of dominant-negative CREB leads to increased mortality and mitochondrial dysfunction in female mice. Am J Physiol Heart Circ Physiol. 2010; 299:H2056–2068. [PubMed: 20935148]
32. Patten IS, Rana S, Shahul S, et al. Cardiac angiogenic imbalance leads to peripartum cardiomyopathy. Nature. 2012; 485:333–338. [PubMed: 22596155]
33. Lehman JJ, Barger PM, Kovacs A, Saffitz JE, Medeiros DM, Kelly DP. Peroxisome proliferator-activated receptor gamma coactivator-1 promotes cardiac mitochondrial biogenesis. J Clin Invest. 2000; 106:847–856. [PubMed: 11018072]
34. Sihag S, Cresci S, Li AY, Sucharov CC, Lehman JJ. PGC-1alpha and ERRalpha target gene downregulation is a signature of the failing human heart. J Mol Cell Cardiol. 2009; 46:201–212. [PubMed: 19061896]
35. Mery PF, Brechler V, Pavoine C, Pecker F, Fischmeister R. Glucagon stimulates the cardiac Ca2+ current by activation of adenylyl cyclase and inhibition of phosphodiesterase. Nature. 1990; 345:158–161. [PubMed: 2159595]
36. Ali S, Ussher JR, Baggio LL, Kabir MG, Charron MJ, Ilkayeva O, Newgard CB, Drucker DJ. Cardiomyocyte glucagon receptor signaling modulates outcomes in mice with experimental myocardial infarction. Mol Metab. 2015; 4:132–143. [PubMed: 25685700]
37. Herzig S, Long F, Jhala US, Hedrick S, Quinn R, Bauer A, Rudolph D, Schutz G, Yoon C, Puigserver P, Spiegelman B, Montminy M. CREB regulates hepatic gluconeogenesis through the coactivator PGC-1. Nature. 2001; 413:179–183. [PubMed: 11557984]
38. Koo SH, Flechner L, Qi L, Zhang X, Screaton RA, Jeffries S, Hedrick S, Xu W, Boussouar F, Brindle P, Takemori H, Montminy M. The CREB coactivator TORC2 is a key regulator of fasting glucose metabolism. Nature. 2005; 437:1109–1111. [PubMed: 16148943]
39. Zhang R, Edwards JR, Ko SY, Dong S, Liu H, Oyajobi BO, Papasian C, Deng HW, Zhao M. Transcriptional regulation of BMP2 expression by the PTH-CREB signaling pathway in osteoblasts. PLoS One. 2011; 6:e20780. [PubMed: 21695256]
40. Hoare SR, Gardella TJ, Usdin TB. Evaluating the signal transduction mechanism of the parathyroid hormone 1 receptor. Effect of receptor-G-protein interaction on the ligand binding mechanism and receptor conformation. J Biol Chem. 2001; 276:7741–7753. [PubMed: 11108715]
41. Avlani VA, Ma W, Mun HC, Leach K, Delbridge L, Christopoulos A, Conigrave AD. Calcium-sensing receptor-dependent activation of CREB phosphorylation in HEK293 cells and human parathyroid cells. Am J Physiol Endocrinol Metab. 2013; 304:E1097–1104. [PubMed: 23531616]

42. Shindo T, Kurihara Y, Nishimatsu H, et al. Vascular abnormalities and elevated blood pressure in mice lacking adrenomedullin gene. Circulation. 2001; 104:1964–1971. [PubMed: 11602502]
43. Caron K, Hagaman J, Nishikimi T, Kim HS, Smithies O. Adrenomedullin gene expression differences in mice do not affect blood pressure but modulate hypertension-induced pathology in males. Proc Natl Acad Sci U S A. 2007; 104:3420–3425. [PubMed: 17360661]
44. Nakamura M, Yoshida H, Makita S, Arakawa N, Niinuma H, Hiramori K. Potent and long-lasting vasodilatory effects of adrenomedullin in humans. Comparisons between normal subjects and patients with chronic heart failure. Circulation. 1997; 95:1214–1221. [PubMed: 9054852]
45. Nagaya N, Satoh T, Nishikimi T, Uematsu M, Furuichi S, Sakamaki F, Oya H, Kyotani S, Nakanishi N, Goto Y, Masuda Y, Miyatake K, Kangawa K. Hemodynamic, renal, and hormonal effects of adrenomedullin infusion in patients with congestive heart failure. Circulation. 2000; 101:498–503. [PubMed: 10662746]
46. Yoshizawa T, Sakurai T, Kamiyoshi A, et al. Novel regulation of cardiac metabolism and homeostasis by the adrenomedullin-receptor activity-modifying protein 2 system. Hypertension. 2013; 61:341–351. [PubMed: 23297372]
47. Weston C, Lu J, Li N, Barkan K, Richards GO, Roberts DJ, Skerry TM, Poyner D, Pardamwar M, Reynolds CA, Dowell SJ, Willars GB, Ladds G. Modulation of Glucagon Receptor Pharmacology by Receptor Activity-modifying Protein-2 (RAMP2). J Biol Chem. 2015; 290:23009–23022. [PubMed: 26198634]
48. Bhashyam S, Fields AV, Patterson B, Testani JM, Chen L, Shen YT, Shannon RP. Glucagon-like peptide-1 increases myocardial glucose uptake via p38alpha MAP kinase-mediated, nitric oxide-dependent mechanisms in conscious dogs with dilated cardiomyopathy. Circ Heart Fail. 2010; 3:512–521. [PubMed: 20466848]
49. Solaro RJ. Is calcium the 'cure' for dilated cardiomyopathy? Nat Med. 1999; 5:1353–1354. [PubMed: 10581071]
50. Polat V, Bozcali E, Uygun T, Opan S, Karakaya O. Low vitamin D status associated with dilated cardiomyopathy. Int J Clin Exp Med. 2015; 8:1356–1362. [PubMed: 25785137]

Novelty and Significance

What Is New?

- Using a novel genetic mouse model, we find that endothelial expression of receptor activity-modifying protein 2 (*Ramp2*) is able to rescue the embryonic lethality of *Ramp2*$^{-/-}$ mice.
- *Ramp2* loss-of-function leads to spontaneous hypotension, dilated cardiomyopathy, and multi-organ inflammation, which we show are not recapitulated in genetic models with loss of calcitonin-receptor-like receptor (CLR) signaling.
- *In vivo* loss of *Ramp2* causes dysregulation of numerous RAMP-associated GPCRs, including the glucagon and parathyroid hormone receptors.

What is Relevant?

- The physiological consequences of RAMP interactions with Family B GPCRs have been challenging to address due to the embryonic lethality of RAMP2 mice. Here, we elucidate the importance of RAMP2 interactions with several GPCR pathways, which can ultimately provide novel targets, or predict off-target consequences, for pharmacological therapies against cardiovascular disease.

Summary

This study provides genetic *in vivo* evidence that endothelial *Ramp2* expression is necessary and sufficient to rescue the lethality of global loss of *Ramp2*. *Ramp2* expression in non-endothelial cells during development is required to maintain adult blood pressure and cardiac homeostasis—a process that involves numerous GPCR signaling pathways, including glucagon and parathyroid hormone receptor signaling. Collectively, these studies extend the functional repertoire of RAMP-associated receptors in cardiovascular physiology.

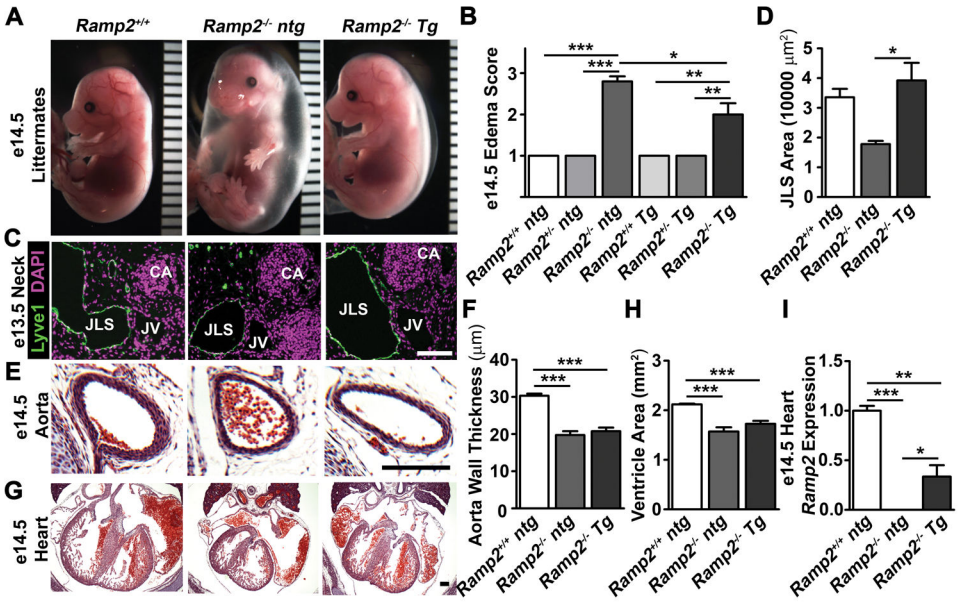

Figure 1. Endothelial restoration of *Ramp2* partially rescues embryonic edema leading to prolonged survival of Ramp2$^{-/-}$ mice

(A) Representative images and **(B)** quantification of edema severity from e14.5 *Ramp2*$^{+/+}$, *Ramp2*$^{-/-}$ *ntg*, and *Ramp2*$^{-/-}$ *Tg* embryos. Edema scoring system: (1) no edema, (2) mild edema, and (3) severe edema. **(C)** Immunohistochemistry and **(D)** quantification of jugular lymph sac size using Lyve1 (green) and DAPI (magenta). CA, carotid artery; JV, jugular vein; JLS, jugular lymph sac. **(E)** Histology of descending aortas and **(F)** quantification of aortic vSMC wall thickness. **(G)** Heart histology, **(H)** quantification of ventricle area, and **(I)** whole heart relative *Ramp2* expression from viable *Ramp2*$^{+/+}$ *ntg*, *Ramp2*$^{-/-}$ *ntg*, and *Ramp*$^{-/-}$ *Tg* e14.5 embryos. Samples were normalized to *Ramp2*$^{+/+}$ *ntg* and *Gapdh* expression. Scale bars: 100 µm. Data represented as average ± SEM from N = 3–8 mice per genotype. Significance determined by one-way ANOVA with Tukey's Multiple Comparison with *p<0.05, **p<0.01, and ***p<0.001.

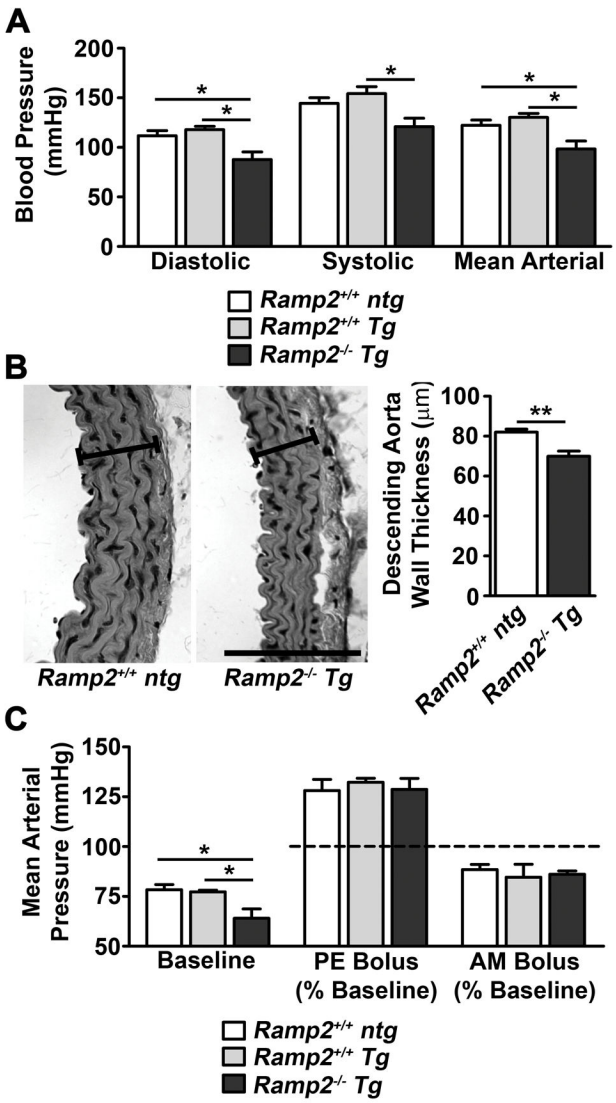

Figure 2. *Ramp2*$^{-/-}$ *Tg* adults are hypotensive

(A) Tail-cuff telemetry blood pressure analysis from conscious *Ramp2*$^{+/+}$ *ntg*, *Ramp2*$^{+/+}$ *Tg*, and *Ramp2*$^{-/-}$ *Tg* adult female mice. **(B)** Representative images and vSMC wall thickness quantifications of *Ramp2*$^{+/+}$ *ntg* and *Ramp2*$^{-/-}$ *Tg* descending aortas. Scale Bars: 100 μm. **(C)** Intra-arterial blood pressure measurements from anesthetized *Ramp2*$^{+/+}$ *ntg*, *Ramp2*$^{+/+}$ *Tg*, and *Ramp2*$^{-/-}$ *Tg* mice during baseline and after challenged with intravenous bolus of 30 μg/kg phenylephrine (PE) or 12 nmol/kg adrenomedullin (AM). Drug response represented as a % change from baseline (dotted line). Data represented as average ± SEM from N = 3–5 mice per genotype. Significance determined by one-way ANOVA with Tukey's Multiple Comparison **(A**, **C)** or unpaired student T-test **(B)** with *p<0.05 and **p<0.01.

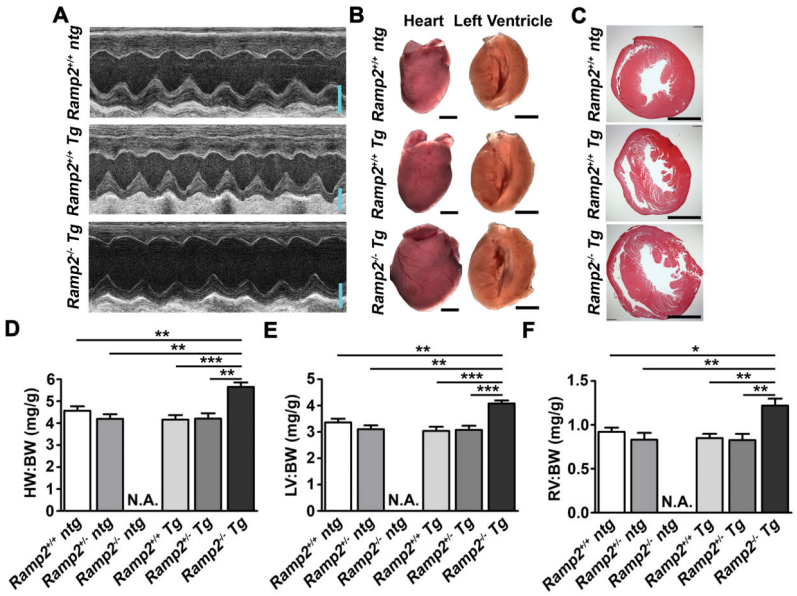

Figure 3. *Ramp2*$^{-/-}$ *Tg* adults develop spontaneous dilated cardiomyopathy

(A) Representative M-mode echocardiograms from left ventricles of *Ramp2*$^{+/+}$ *ntg*, *Ramp2*$^{+/+}$ *Tg*, and *Ramp2*$^{-/-}$ *Tg* mice. Macroscopic **(B)** and H&E **(C)** images of whole hearts and left ventricles from of *Ramp2*$^{+/+}$ *ntg*, *Ramp2*$^{+/+}$ *Tg*, and *Ramp2*$^{-/-}$ *Tg* mice. Scale Bars: 2 mm. Quantification of heart **(D)**, left ventricle **(E)**, and right ventricle **(F)** weight normalized to body weight. Data represented as average ± SEM from N = 4–10 mice per genotype. Significance determined by one-way ANOVA with Tukey's Multiple Comparison with *p<0.05, **p<0.01, ***p<0.001.

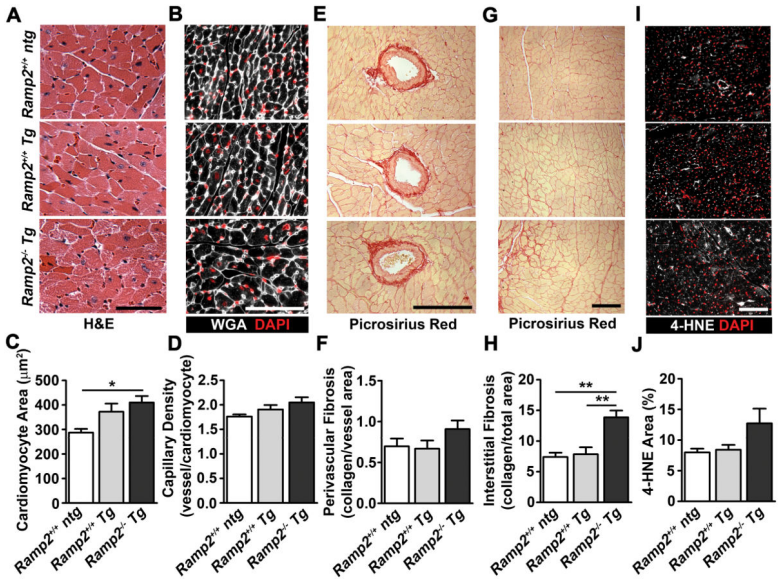

Figure 4. *Ramp2*$^{-/-}$ *Tg* left ventricles hypertrophied with early fibrotic and oxidative stress changes

(A) Histology and **(B)** wheat germ agglutinin (WGA, white) immunohistochemistry showing cardiomyocytes from *Ramp2*$^{+/+}$ *ntg*, *Ramp2*$^{+/+}$ *Tg*, and *Ramp2*$^{-/-}$ *Tg* left ventricles. Quantification of **(C)** cardiomyocyte cross-sectional area and **(D)** capillary density from mouse left ventricles. Representative images and quantification of left ventricles stained with Picrosirius Red showing **(E–F)** perivascular and **(G–H)** interstitial fibrosis/collagen deposition. **(I)** Immunohistochemistry and **(J)** quantification of 4-HNE (white) staining showing relative levels oxidative stress in left ventricles. Scale Bars: 100 μm. Data represented as averages ± SEM from N = 3–4 mice per genotype. Significance determined by one-way ANOVA with Tukey's Multiple Comparison with *p<0.05 and **p<0.01.

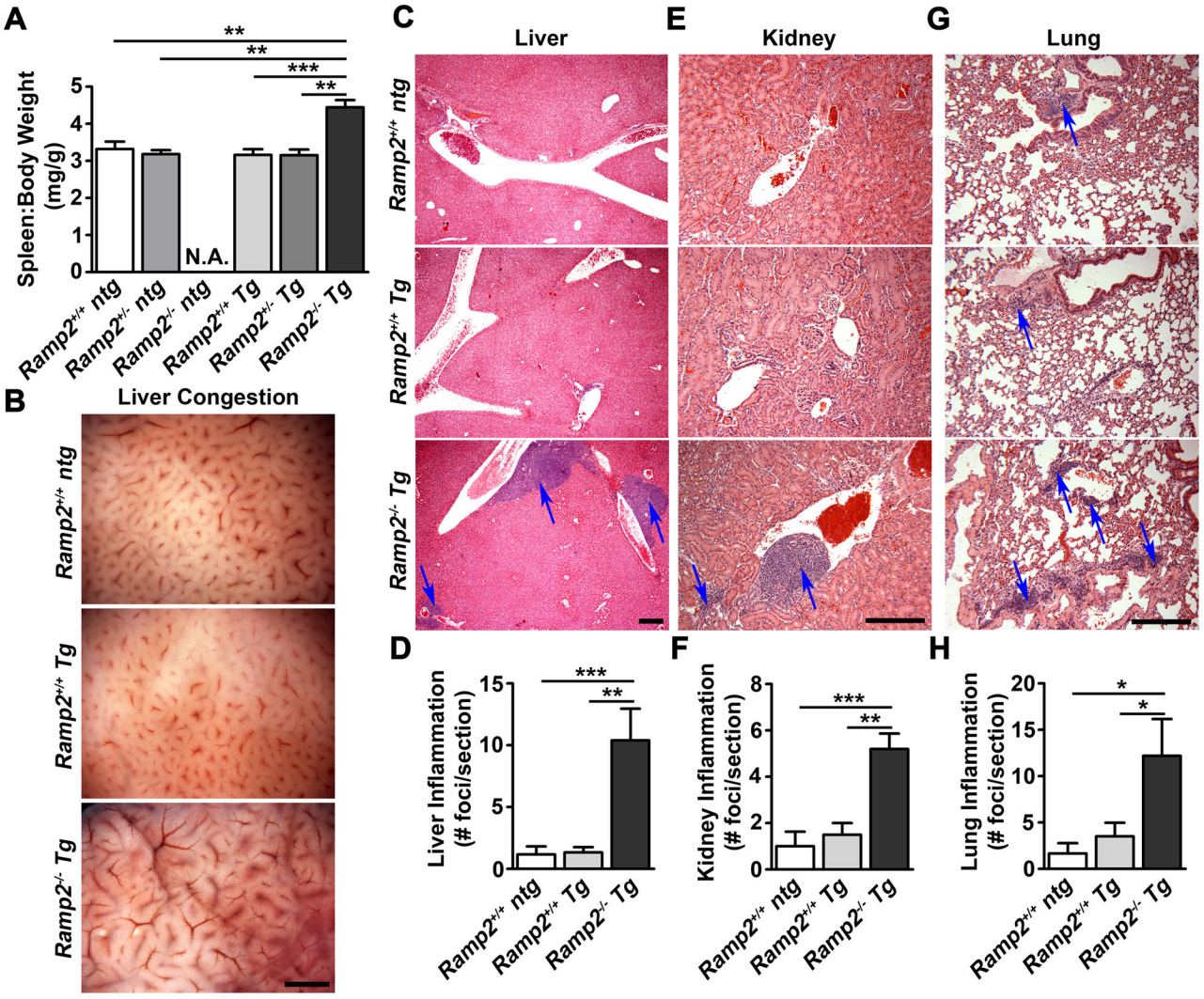

Figure 5. *Ramp2*$^{-/-}$ *Tg* have vascular congestion and multi-organ inflammation downstream of hypotension and dilated cardiomyopathy

(A) Spleen to body weight ratio from *Ramp2*$^{+/+}$, *Ramp2*$^{+/-}$, and *Ramp2*$^{-/-}$ females with and without the transgene. **(B)** Macroscopic images of liver vasculature abnormalities in *Ramp2*$^{-/-}$ *Tg* compared to that of *Ramp2*$^{+/+}$ *ntg* and *Ramp2*$^{+/+}$ *Tg* controls. Histology and quantification of inflammatory foci (blue arrows) in **(C–D)** livers, **(E–F)** kidneys, and **(G–H)** lungs from *Ramp2*$^{+/+}$ *ntg*, *Ramp2*$^{+/+}$ *Tg*, and *Ramp2*$^{-/-}$ *Tg* mice. Scale Bars: 1 mm **(B)** and 100 μm **(C, E, G)**. Data represented as averages ± SEM from N = 3–4 mice per genotype. Significance determined by one-way ANOVA with Tukey's Multiple Comparison with *p<0.05, **p<0.01, ***p<0.001.

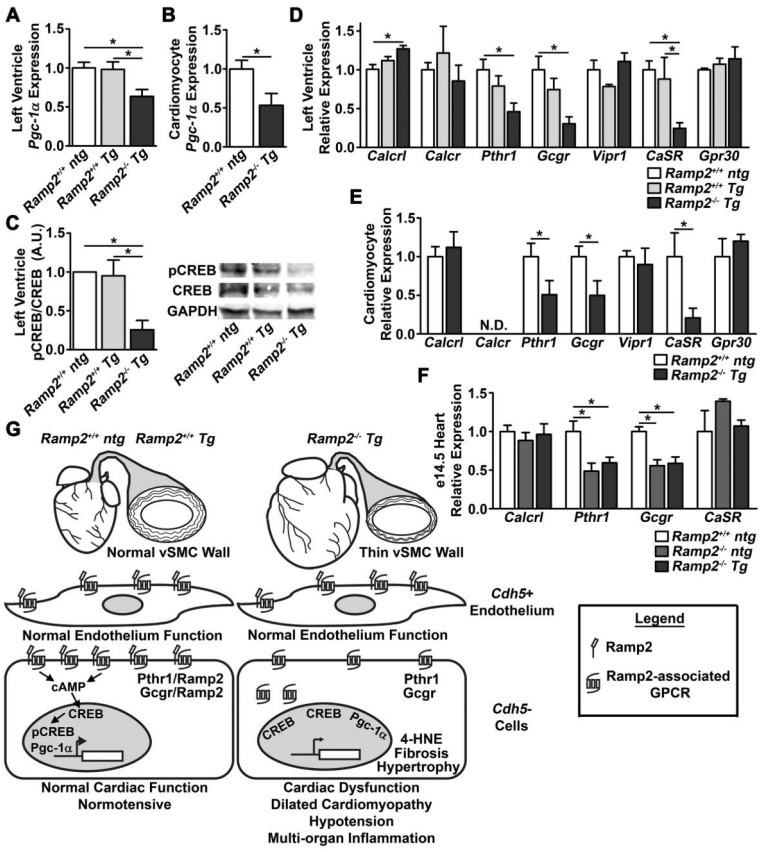

Figure 6. Decreased signaling and expression of RAMP-associated GPCRs in embryonic and adult *Ramp2*$^{-/-}$ *Tg* hearts

RT-PCR showing relative *Pgc-1α* expression from *Ramp2*$^{+/+}$ *ntg*, *Ramp2*$^{+/+}$ *Tg, and Ramp2*$^{-/-}$ *Tg* adult left ventricle **(A)** or cardiomyocytes **(B). (C)** Quantification and representative western blot of phosphorylated CREB to total CREB in *Ramp2*$^{+/+}$ ntg, *Ramp2*$^{+/+}$ *Tg, and Ramp2*$^{-/-}$ *Tg* left ventricles. Samples were normalized to *Ramp2*$^{+/+}$ *ntg* and CREB with Gapdh used as a loading control. Relative expression of the Family B GPCRs; *Calcrl*, *Calcr*, *Pthr1*, *Gcgr*, *Vipr1*, *CaSR* and *Gpr30* in **(D)** whole left ventricles and **(E)** isolated cardiomyocytes from adult *Ramp2*$^{-/-}$ *Tg* mice and *Ramp2*$^{+/+}$ controls. **(F)** Relative GPCR expression from e14.5 *Ramp2*$^{+/+}$ *ntg*, *Ramp2*$^{-/-}$ *ntg*, and *Ramp2*$^{-/-}$ *Tg* whole hearts. Samples were normalized to *Ramp2*$^{+/+}$ *ntg* and *Gapdh* and *Rpl19* expression. **(E)** Data represented as averages ± SEM from N = 3–5 mice per genotype. Significance determined by one-way ANOVA with Tukey's Multiple Comparison **(A, C, D, F)** or unpaired student T-test **(B, E)** with *p<0.05. **(F)** Model summarizing cardiovascular phenotypes in *Cdh5*+ endothelium and *Cdh5*- cells in *Ramp2*$^{+/+}$ *ntg*, *Ramp2*$^{+/+}$ *Tg*, and *Ramp2*$^{-/-}$ *Tg* adults.

Table 1

Endothelial restoration of *Ramp2* can rescue the global *Ramp2*$^{-/-}$ embryonic lethality

Breeding results, both expected Mendelian and actual results from *Ramp2*$^{+/-}$ *Tg(Cdh5-Ramp2)* crossed with *Ramp2*$^{+/-}$ *ntg*. N = 280 pups.

				Tg(Cdh5-Ramp2)		
Mendelian Ratio	***Ramp2*$^{+/+}$**	***ntg Ramp2*$^{+/-}$**	***Ramp2*$^{-/-}$**	***Ramp2*$^{+/+}$**	***Ramp2*$^{+/-}$**	***Ramp2*$^{-/-}$**
Expected N	35	70	35	35	70	35
Actual N P7	47	88	0	48	83	14*
Actual/Expected	134%	126%	0%	137%	119%	40%

Significance in survival between *Ramp2*$^{-/-}$ *ntg* and *Ramp2*$^{-/-}$ *Tg* pups determined by the Mantel-Cox test:

*p<0.001.

Hypertension. Author manuscript; available in PMC 2017 September 01.

Table 2

***Ramp2*$^{-/-}$ *Tg* adults develop left ventricle dilatation and declining heart function**

Echocardiography analysis from *Ramp2*$^{+/+}$, *Ramp2*$^{+/-}$, and *Ramp2*$^{-/-}$ mice with and without the transgene.

Echo Parameters	*ntg*		*Tg (Cdh5-Ramp2)*		
	Ramp2$^{+/+}$	*Ramp2*$^{+/-}$	*Ramp2*$^{+/+}$	*Ramp2*$^{+/-}$	*Ramp2*$^{-/-}$
Mouse Number	10	4	7	4	7
Mouse Age (wks)	26.7±1.3	26.8±2.0	29.3±2.3	26.3±2.2	29.7±1.6
Heart Rate (BPM)	624±15	578±38	574±50	614±55	552±21
LV Vol, d (μL)	35.6±4.7	32.0±3.9	34.1±6.7	27.9± 5.9	73.4±9.5 *,†,‡,§
LV Vol, s μL)	7.6±1.6	5.0±1.4	7.0±2.7	5.4±2.4	23.1±3.5 *,†,‡,§
CO (mL/min)	16.5±2.1	15.4±1.2	16.1±3.2	13.2±0.9	27.0±4.8 *
EF (%)	81.2±3.0	85.1±2.0	82.4±3.6	83.3±5.1	68.3±2.3 *,†,‡,§
FS (%)	51.6±2.7	52.9±2.2	51.1±4.0	52.4±6.5	37.9±1.8 *,‡
IVS, s (mm)	1.13±0.05	1.16±0.06	1.12±0.07	1.07±0.07	1.08±0.07
IVS, s (mm)	1.72±0.06	1.74±0.06	1.73±0.07	1.68±0.13	1.60±0.07
LVID, d (mm)	2.94±0.20	2.88±0.14	2.90±0.22	2.70±0.23	4.03±0.22 *,†,‡,§
LVID, s (mm)	1.52±0.17	1.36±0.13	1.45±0.21	1.32±0.27	2.50±0.14 *,†,‡,§
LVPW, d (mm)	1.54±0.10	0.96±0.07	1.22±0.13	1.08±0.30	0.87±0.06
LVPW, s (mm)	1.74±0.13	1.72±0.04	1.76±0.08	1.60±0.20	1.40±0.08

BPM, beats per minute; LV, left ventricle; d, diastole; s, systole; CO, cardiac output; EF, ejection fraction; FS, fractional shortening; IVS, interventricular septal; LVID, left ventricle internal diameter; LVPW, left ventricle posterior wall. Data represented as averages ± SEM with significance of $p<0.05$ determined by one-way ANOVA with Tukey's Multiple Comparison. Significant compared to:

**Ramp2*$^{+/+}$ *ntg,*

†*Ramp2*$^{+/-}$ *ntg,*

‡*Ramp2*$^{+/+}$ *Tg,*

§*Ramp2*$^{+/-}$ *Tg.*